Stimulus-frequency-emission group delay: A test of coherent reflection filtering and a window on cochlear tuning

Christopher A. Shera[a] and John J. Guinan, Jr.
Eaton-Peabody Laboratory of Auditory Physiology, Massachusetts Eye and Ear Infirmary, 243 Charles Street, Boston, Massachusetts 02114 and Department of Otology and Laryngology, Harvard Medical School, Boston, Massachusetts 02115

(Received 4 October 2002; accepted for publication 13 January 2003)

This paper tests and applies a key prediction of the theory of coherent reflection filtering for the generation of reflection-source otoacoustic emissions. The theory predicts that reflection-source-emission group delay is determined by the group delay of the basilar-membrane (BM) transfer function at its peak. This prediction is tested over a seven-octave frequency range in cats and guinea pigs using measurements of stimulus-frequency-emission (SFOAE) group delay. A comparison with group delays calculated from published measurements of BM mechanical transfer functions supports the theory at the basal end of the cochlea. A comparison across the whole frequency range based on variations in the sharpness of neural tuning with characteristic frequency (CF) suggests that the predicted relation holds in the basal-most 60% of the cochlea. At the apical end of the cochlea, however, the measurements disagree with neural and mechanical group delays. This disagreement suggests that there are important differences in cochlear mechanics and/or mechanisms of emission generation between the base and apex of the cochlea. Measurements in humans over a four-octave range indicate that human SFOAE group delays are roughly a factor of 3 longer than their counterparts in cat and guinea pig but manifest similar trends across CF. The measurements thus reveal global deviations from scaling whose form appears quantitatively similar in all three species. Interpreted using the theory of coherent reflection filtering, the group delay measurements indicate that the wavelength at the peak of the traveling wave decreases with increasing CF at a rate of roughly 25% per octave in the base of the cochlea. The measurements and analysis reported here illustrate the rich potential inherent in OAE measurements for obtaining valuable information about basic cochlear properties such as tuning. [DOI: 10.1121/1.1557211]

PACS numbers: 43.64.Bt, 43.64.Kc, 43.64.Jb [LHC]

I. INTRODUCTION

The theory of coherent reflection filtering (Shera and Zweig, 1993b; Zweig and Shera, 1995) relates ear-canal otoacoustic measurements to the mechanical response of the organ of Corti, providing a quantitative theoretical foundation for the use of otoacoustic emissions as noninvasive probes of cochlear mechanics. The theory indicates that reflection-source otoacoustic emissions [such as stimulus-frequency emissions, or SFOAEs, evoked at low sound levels (Shera and Guinan, 1999)] arise via coherent reflection from densely and ''randomly'' distributed cochlear impedance perturbations. These perturbations may include spatial variations in outer-hair-cell (OHC) number and geometry (e.g., Engström *et al.*, 1966; Bredberg, 1968; Wright, 1984; Lonsbury-Martin *et al.*, 1988) and/or perturbations not clearly visible in conventional anatomical preparations, such as variations in OHC forces due to random, cell-to-cell variations in the number of somatic motor proteins.

Among the theory's many predictions and applications (e.g., Zweig and Shera, 1995; Talmadge *et al.*, 1998) is one of special relevance to the noninvasive measurement of cochlear tuning. Specifically, the theory predicts that reflection-source-emission group delay is determined by the group delay of the basilar-membrane (BM) mechanical transfer function at its peak. Since BM transfer functions at low levels manifest many of the characteristics of minimum-phase-shift filters (e.g., Zweig, 1976; de Boer, 1997), their bandwidths and phase slopes (i.e., group delays) are related, with sharper tuning corresponding to longer group delays. If the theory's prediction about reflection-source-emission group delay is correct, otoacoustic measurements can be used to provide a noninvasive measure of basilar-membrane group delay, and, hence, indirectly, of the frequency selectivity of cochlear tuning. In this paper we test the predicted relation between otoacoustic and BM group delays;[1] we apply these ideas to estimate the frequency selectivity of cochlear tuning in another publication (Shera *et al.*, 2002).

II. RELATING SFOAE AND BM GROUP DELAYS

The theory of coherent reflection filtering predicts that the SFOAE group delay, $\tau_{\mathrm{SFOAE}}(f)$, is approximately equal to twice the group delay of the basilar-membrane (BM) mechanical transfer function, evaluated at the cochlear location with CF equal to the stimulus frequency:

$$\tau_{\mathrm{SFOAE}}(f) \approx 2\,\hat{\tau}_{\mathrm{BM}}(f), \tag{1}$$

where $\hat{\tau}_{\mathrm{BM}}(f) = \tau_{\mathrm{BM}}[x_{\mathrm{CF}}(f), f]$. The factor of two arises be-

[a]Electronic mail: shera@epl.meei.harvard.edu

 0001-4966/2003/113(5)/2762/11/$19.00

cause reflection-source-emission group delay depends on round-trip wave travel. Derived in the next section,[2] Eq. (1) is the central relation about which the arguments of this paper revolve.

A. Computing the round-trip travel time

To derive Eq. (1) from the theory of coherent reflection filtering we approximate SFOAE group delay $\tau_{\mathrm{SFOAE}}(f)$ by the round-trip wave travel time $\tau_{\rightleftarrows}(x_{\mathrm{ref}},f)$ between the stapes and the region of reflection, assumed centered about an as yet unspecified point, $x_{\mathrm{ref}}(f)$. Since emissions at different frequencies may arise from different cochlear locations, we write $x_{\mathrm{ref}}(f)$ as an explicit function of frequency. The identification of emission group delay with cochlear round-trip travel times neglects contributions to $\tau_{\mathrm{SFOAE}}(f)$ introduced by eardrum transduction and subsequent transmission through the middle ear.[3] Measurements indicate that delays due to round-trip middle-ear transmission are small; in cat and gerbil they amount to approximately 50 μs, or only about 1 cycle at 20 kHz (Puria and Allen, 1998; Olson, 1998).

We compute the round-trip wave travel time by dividing the total distance into segments of length Δx and adding up the times required to traverse each segment. Taking the limit as $\Delta x \rightarrow 0$ yields the integral

$$\tau_{\mathrm{SFOAE}}(f) \approx \tau_{\rightleftarrows}[x_{\mathrm{ref}}(f),f] = 2\int_0^{x_{\mathrm{ref}}(f)} \frac{dx}{v(x,f)}, \tag{2}$$

where $v(x,f)$ is the group velocity at location x of waves of frequency f traveling along the cochlear spiral. The reciprocal of the group velocity is given by (e.g., Brillouin, 1946)

$$v^{-1} = \frac{1}{2\pi}\frac{\partial k}{\partial f}, \tag{3}$$

where the (real-valued) wavenumber $k(x,f)$ is 2π divided by the local wavelength [i.e., $2\pi/\lambda(x,f)$]. The wavenumber is related to the spatial derivative of the phase of the traveling wave through the equation

$$k(x,f) = -\frac{\partial \angle T}{\partial x}, \tag{4}$$

where $T(x,f)$ is the traveling wave at frequency f. Written in terms of its amplitude and phase, T has the form $T = |T|e^{i\angle T}$.

1. The region of reflection

According to the theory of coherent reflection filtering, reflection-source OAEs arise by reflection off densely and irregularly distributed cochlear impedance perturbations. At all frequencies the net backward-traveling wave is dominated by wavelets reflected within the region about the peak of the traveling wave, where the wave amplitude is much larger than it is elsewhere. The centroid of the scattering region, $x_{\mathrm{ref}}(f)$, is then the characteristic place for frequency f. In other words,

$$x_{\mathrm{ref}}(f) = x_{\mathrm{CF}}(f) \equiv \hat{x}(f), \tag{5}$$

where the diacritical hat denotes the peak of the traveling wave. Other models of reflection-source OAEs predict no such effective localization of the reflection to the region about the peak. For example, many models assume only sparse, isolated impedance discontinuities (e.g., Kemp, 1980, 1986; Zwicker, 1989); in such models reflection occurs at the site of the discontinuity, which coincides with the peak region only at certain frequencies. In other models, such as Strube's (1989), the perturbations are dense but quasi-sinusoidally distributed; reflection is then largely localized to the region where the wavelength of the traveling wave matches twice the spatial period of the assumed periodic distribution.

2. Finding the group delay

Combining Eqs. (2)–(5) yields

$$\tau_{\mathrm{SFOAE}}(f) \approx -2\int_0^{\hat{x}(f)} \frac{1}{2\pi}\frac{\partial}{\partial f}\frac{\partial \angle T}{\partial x}\,dx. \tag{6}$$

Continuity guarantees the equality of mixed partials (e.g., Apostol, 1969), so we interchange the order of differentiation in the integrand to obtain

$$\tau_{\mathrm{SFOAE}}(f) \approx -2\int_0^{\hat{x}(f)} \frac{\partial}{\partial x}\frac{1}{2\pi}\frac{\partial \angle T}{\partial f}\,dx$$

$$= 2\int_0^{\hat{x}(f)} \frac{\partial \tau_{\mathrm{BM}}}{\partial x}\,dx, \tag{7}$$

where we have used the definition of the traveling-wave group delay,

$$\tau_{\mathrm{BM}}(x,f) = -\frac{1}{2\pi}\frac{\partial \angle T}{\partial f}. \tag{8}$$

Evaluating the integral yields

$$\tau_{\mathrm{SFOAE}}(f) \approx 2\{\tau_{\mathrm{BM}}[\hat{x}(f),f)] - \tau_{\mathrm{BM}}(0,f)\}. \tag{9}$$

Since the wave speed slows considerably as it approaches the peak location (e.g., Lighthill, 1981), contributions to the travel time coming from the lower limit of integration can be neglected. We thus obtain the relation given above as Eq. (1):

$$\tau_{\mathrm{SFOAE}}(f) \approx 2\,\hat{\tau}_{\mathrm{BM}}(f), \tag{10}$$

where $\hat{\tau}_{\mathrm{BM}}(f) = \tau_{\mathrm{BM}}[\hat{x}(f),f]$.

In the above derivation we have regarded $T(x,f)$ as the traveling wave (i.e., as a function of x at fixed f). Local scaling symmetry implies that the same function $T(x,f)$ also represents the BM transfer function as a function of f at fixed x. Scaling therefore implies that empirical estimates of the traveling-wave group delay $\hat{\tau}_{\mathrm{BM}}(f)$ appearing in Eq. (1) can be obtained from measurements of the slope of the phase of BM transfer function near its peak.

III. MEASUREMENTS OF SFOAE GROUP DELAY IN THREE SPECIES

To test Eq. (1) we measured SFOAE phase over a seven-octave frequency range in two species widely used as models of mammalian hearing (cat and guinea pig). For comparison,

and for application to noninvasive estimates of cochlear tuning (cf. Shera *et al.*, 2002), we made measurements spanning four and a half octaves in humans.

A. Measurement methods

The methods and equipment used to measure SFOAEs were generally similar to those detailed previously (Shera and Guinan, 1999; Guinan, 1986). Briefly, we measured SFOAEs in guinea pigs ($n=9$) and humans ($n=9$) using a variant of the acoustic suppression method (Shera and Guinan, 1999) and in cats using either acoustic ($n=3$) or efferent ($n=5$) suppression (Guinan, 1986). In both methods, the emission is obtained as the complex (or vector) difference between the ear-canal pressure at the probe frequency measured first with the probe tone alone and then with the addition of a ''suppressor.'' The suppressor was either (1) an acoustic suppressor tone at a nearby frequency or (2) olivocochlear efferent stimulation via electrical shocks applied at the floor of the fourth ventricle. Both acoustic and efferent suppression are assumed to reduce the SFOAE at the probe frequency substantially. In all cases, probe level was approximately 40 dB SPL in the ear canal. Measurements were made versus probe frequency over at least a four-octave range with a frequency resolution sufficient to prevent ambiguities in phase unwrapping. Emission group delays, τ_{SFOAE}—defined as the negative slope of the emission-phase (in cycles) versus frequency function—were calculated from unwrapped phase responses using centered differences (e.g., Press *et al.*, 1992). Only group delays at frequencies where the emission amplitude was at least 15 dB above the measurement noise floor (typically -25 dB SPL) are included in the final data set. Since no significant differences between the delays measured using acoustic and efferent suppression were found, data from the two techniques were pooled. Details of animal care and preparation are discussed elsewhere (Guinan, 1986; Shera *et al.*, 2000). Treatment of animal and human subjects accorded with protocols established at the Massachusetts Eye and Ear Infirmary.

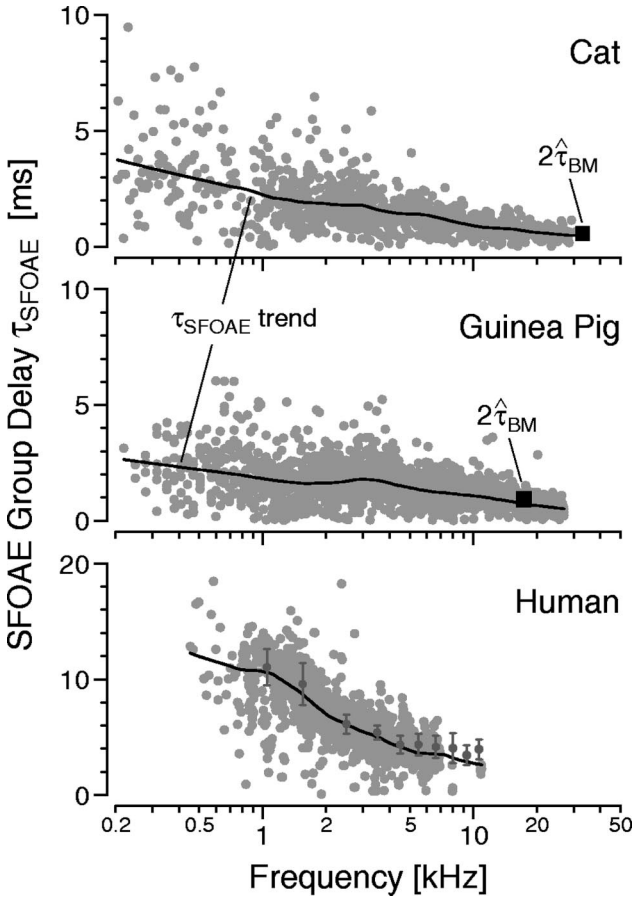

FIG. 1. Stimulus-frequency emission group delay, $\tau_{\mathrm{SFOAE}}(f)$, versus frequency in three species. The data are shown as a scatterplot (gray dots) together with loess trend lines (Cleveland, 1993) computed from the data (solid lines). Human SFOAE data from Dreisbach *et al.* (1998) are included to supplement our data at high frequencies (dots with error bars representing standard deviations). The black squares (■) provide a test of Eq. (1) in cat and guinea pig by showing values of $2\hat{\tau}_{\mathrm{BM}}$ computed from published measurements of BM mechanical transfer functions in the same species (Cooper and Rhode, 1992; Nuttall and Dolan, 1996). Like the SFOAE measurements shown here, the BM measurements were made in healthy preparations at stimulus levels of roughly 40 dB SPL. Note the difference in vertical scale between the human and animal graphs; human group delays are roughly a factor of 3 larger than those in cat and guinea pig.

B. Empirical SFOAE group delays

Figure 1 show scatterplots of our measurements of $\tau_{\mathrm{SFOAE}}(f)$ in three species together with loess trend lines (Cleveland, 1993) to guide the eye. The group delay $\tau_{\mathrm{SFOAE}}(f)$ decreases with increasing frequency, a dispersive trend consistent with time-domain measurements of the latency of click- and tone-burst-evoked emissions (e.g., Kemp, 1978; Wilson, 1980; Norton and Neely, 1987; Sisto and Moleti, 2002). For each frequency, SFOAE group delays in human are roughly a factor of 3 larger than in cat and guinea pig (see also Zwicker and Manley, 1981).

1. Origin of the variability

Although the trend line is robust both between and within individual subjects, the data points show considerable scatter. This scatter does not arise from measurement noise; indeed, the measurements are quite reproducible in each subject. Rather, the scatter comes from intrinsic variations in emission phase that are correlated with variations in emission amplitude across frequency. Intrinsic variations in emission amplitude and phase are predicted by the theory of coherent reflection filtering. To understand their origin, note that the theory indicates that SFOAEs are analogous to ''bandpass-filtered noise'' (Zweig and Shera, 1995). In this analogy, the ''noise'' is the irregular spatial arrangement and strength of the impedance perturbations that scatter the wave, and the ''bandpass filter'' results from interference among the multiple wavelets originating from the scattering region (Zweig and Shera, 1995). Unlike distortion-source emissions, whose amplitudes and phases typically vary relatively slowly with frequency, reflection-source emissions often vary considerably with frequency. For example, SFOAE amplitude spectra are often punctuated by relatively sharp notches (e.g., Fig. 9 of Shera and Guinan, 1999). According to the model, such notches result from random spatial fluctuations in the irregularities that scatter the wave. At some frequencies, wavelets scattered from different locations within the scattering region combine nearly out of phase, resulting in near cancellation of the net reflected wave.

Along with these large and small scale amplitude variations come corresponding phase variations whose effect is magnified here by taking the frequency derivative to compute the group delay.

C. Testing the predicted relation at high frequencies

We test the predicted relation [Eq. (1)] by overlaying in Fig. 1 values of $2\hat{\tau}_{\mathrm{BM}}$ computed from published measurements of basilar-membrane motion in the cat and guinea pig. Like the SFOAE measurements reported here, the BM measurements shown for comparison were made in healthy preparations at stimulus levels of roughly 40 dB SPL. Although the BM data are limited to high CFs, and to a single animal in each species, the agreement in the figure appears good in both cat and guinea pig. Computing the ratio $\tau_{\mathrm{SFOAE}}/\hat{\tau}_{\mathrm{BM}}$ allows a more quantitative comparison. The calculations yield ratios of 1.7 ± 0.2 in the cat and 1.6 ± 0.3 in the guinea pig,[4] where the error bars represent nominal 95% confidence intervals based on the uncertainties arising from the estimates of phase slope. In both species, the empirical ratios $\tau_{\mathrm{SFOAE}}/\hat{\tau}_{\mathrm{BM}}$, although significantly greater than 1, are smaller than the value 2 predicted by the theory. Note, however, that the confidence intervals given here underestimate the actual uncertainties because they do not include contributions arising from the variation in $\hat{\tau}_{\mathrm{BM}}$ between animals. Additional data are therefore needed to assess the differences among preparations and determine whether there are systematic deviations from the theoretical relation $\tau_{\mathrm{SFOAE}}\approx 2\hat{\tau}_{\mathrm{BM}}$.

IV. RELATING SFOAE GROUP DELAY TO COCHLEAR TUNING

Although SFOAE group delays are readily measured over a wide frequency range (see Fig. 1), direct comparisons between SFOAE and BM group delays are currently constrained to those few locations for which access to the basilar membrane can be obtained without significant loss of cochlear function (e.g., the squares in Fig. 1). To test whether SFOAE delays are consistent with the predictions of Eq. (1) over a broader region of the cochlea, we explore the relation between SFOAE group delay and cochlear tuning, as assessed using auditory-nerve-fiber (ANF) tuning curves.

We base our approach on the observation that at low sound levels the tuning of the basilar membrane appears nearly identical to the tuning of corresponding auditory-nerve fibers at frequencies in the tip region near CF (Narayan *et al.*, 1998). Although systematic measures of ANF group delay are not available in the basal half of the cochlea—the loss of phase locking above a few kilohertz means that cochlear phase characteristics cannot readily be obtained at high frequencies from ANF responses to tones or noise[5]—measurements of cochlear frequency selectivity are easily obtained from threshold tuning curves over the entire range of hearing. We relate BM group delay to cochlear-filter bandwidth by noting that at low levels BM transfer functions manifest many of the characteristics of minimum-phase-shift filters (e.g., Zweig, 1976; de Boer, 1997). In particular, their bandwidths and phase slopes are reciprocally related, with smaller bandwidths corresponding to steeper phase slopes (i.e., longer delays).

A. Dimensionless measures of tuning bandwidth and group delay

Our two measures of cochlear tuning—bandwidth and group delay—have different units (frequency and time, respectively). To compare them we render them dimensionless by normalizing each by the corresponding natural units of frequency and/or time. For the bandwidth, the natural frequency unit is the local characteristic frequency, f_{CF}. We therefore represent cochlear frequency selectivity using the parameter-free measure Q_{ERB}, defined as

$$Q_{\mathrm{ERB}}(f_{\mathrm{CF}}) \equiv f_{\mathrm{CF}}/\mathrm{ERB}(f_{\mathrm{CF}}), \tag{11}$$

where ERB is the equivalent rectangular bandwidth (i.e., the bandwidth of the rectangular filter with the same peak amplitude that passes the same total power).[6] Q_{ERB} is a measure of the "sharpness" of tuning: the smaller the bandwidth, the larger the Q_{ERB}. For the BM group delay, the natural unit of time is the reciprocal of the characteristic frequency. We define $N_{\mathrm{BM}}(f_{\mathrm{CF}})$ as

$$N_{\mathrm{BM}}(f_{\mathrm{CF}}) \equiv f_{\mathrm{CF}} \cdot \hat{\tau}_{\mathrm{BM}}(f_{\mathrm{CF}}). \tag{12}$$

$N_{\mathrm{BM}}(f_{\mathrm{CF}})$ is simply the group delay measured in periods of the characteristic frequency. In an analogous fashion we define the dimensionless SFOAE group delay by measuring time in periods of the stimulus frequency: $N_{\mathrm{SFOAE}}(f) \equiv f \cdot \tau_{\mathrm{SFOAE}}(f)$. Equation (1) implies that

$$\boxed{N_{\mathrm{SFOAE}}(f) \approx 2N_{\mathrm{BM}}(f).} \tag{13}$$

B. Frequency dependence of cochlear tuning

Figure 2 shows ANF-derived values of $Q_{\mathrm{ERB}}(f_{\mathrm{CF}})$ in cat and guinea pig. The figure illustrates that the sharpness of cochlear tuning increases gradually with CF throughout the cochlea. Although close examination of the data suggests a possible flattening of the Q_{ERB} at the highest CFs, this trend may well be a measurement artifact. Mechanical responses in the high-frequency region of the cochlea are extremely labile, and cochlear tuning at high CFs can easily be damaged (e.g., as a result of trauma caused by surgically opening the auditory bulla). As illustrated in the figure, power-law fits (straight lines on log-log axes) provide an excellent description of the overall trends in the data. Parameters for the fits are given in Table I.

C. Expected covariation of tuning bandwidth and group delay

Because bandwidth and group delay are inversely related, the product of the two (i.e., the "tuning ratio" $N_{\mathrm{BM}}/Q_{\mathrm{ERB}}$) is likely to vary more slowly along the cochlea than does either factor by itself. Consider, for example, representing BM tuning by a minimum-phase band-pass filter (e.g., a gammatone filter) of center frequency f_{CF}. Denote the filter bandwidth (e.g., the ERB) by Δf. If the filter phase

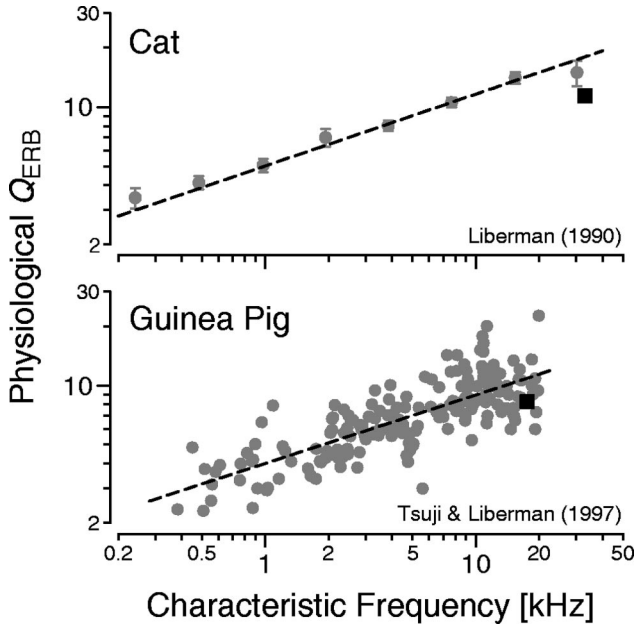

FIG. 2. Physiological values of Q_{ERB} in cat and guinea pig. In guinea pig, values of Q_{ERB} were computed from high-spontaneous-rate (high-SR) ANF threshold tuning curves (Tsuji and Liberman, 1997) using standard algorithms (Evans and Wilson, 1973). Since original tuning curves were unavailable in cat, the approximate proportionality between Q_{ERB} and Q_{10} discussed in footnote 6 was used to convert measurements of Q_{10} in high-SR fibers (Liberman, 1990) to corresponding values of Q_{ERB}. The cat data represent means and their standard errors in eight logarithmically spaced frequency bins. The dashed lines give power-law fits to the data (parameters in Table I). Shown for comparison are Q_{ERB} values (■) computed from the magnitudes of the mechanical transfer functions whose group delays appear in Fig. 1 (Cooper and Rhode, 1992; Nuttall and Dolan, 1996).

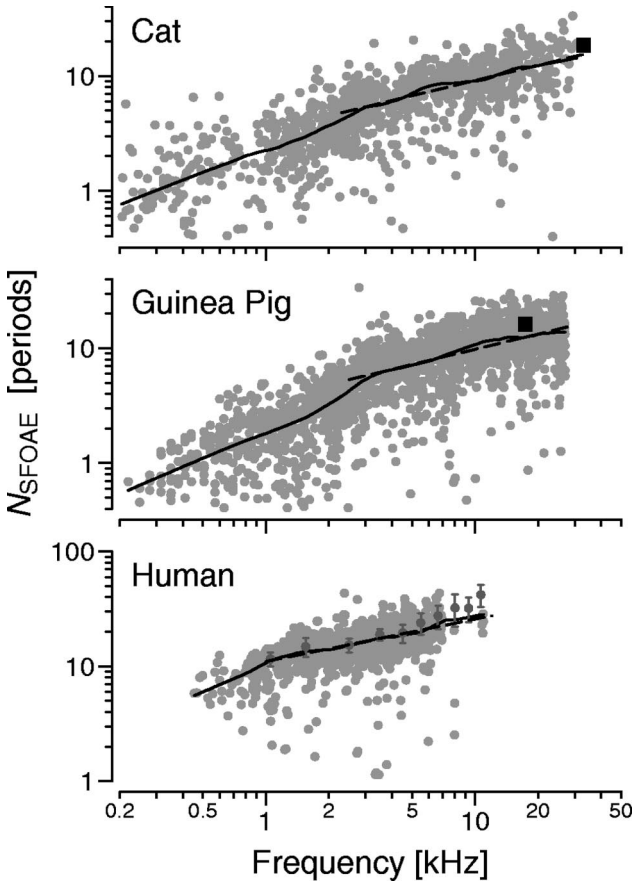

FIG. 3. N_{SFOAE} versus frequency in three species. The group-delay data (gray dots) and trends (solid lines) from Fig. 1 are replotted in dimensionless form in units of periods of the stimulus frequency. Shown for comparison are power-law fits to the data from roughly the basal-most 60% of the cochlea (dashed lines; parameters in Table I). Note that all vertical scales span two decades. Comparison with Fig. 2 demonstrates that in cats and guinea pigs the frequency dependence of $N_{SFOAE}(f)$ generally parallels the CF-dependence of the sharpness of tuning, at least in the basal half of the cochlea.

lag increases by an amount $|\Delta\phi|$ (in cycles) over the bandwidth Δf (in Hz), then the filter group delay is approximately $\hat{\tau}_{BM} \approx |\Delta\phi|/\Delta f$. The value of N_{BM}/Q_{ERB} is therefore[7]

$$N_{BM}/Q_{ERB} = \frac{\hat{\tau}_{BM} \cdot f_{CF}}{f_{CF}/\Delta f} = \hat{\tau}_{BM}\,\Delta f \approx |\Delta\phi|. \tag{14}$$

In other words, the tuning ratio N_{BM}/Q_{ERB} is simply the phase change (in cycles) across the filter bandwidth Δf. In filters of fixed type and order this phase change is largely independent of bandwidth. Since the shapes of neural tuning curves change relatively slowly with CF in the basal half of the cochlea (Liberman, 1978; Liberman and Kiang, 1978), we therefore expect Q_{ERB} and N_{BM} to vary in almost constant proportion across CF. If this is the case, Eq. (13) relating N_{BM} to N_{SFOAE} implies that Q_{ERB} and N_{SFOAE} will also vary together across CF.

TABLE I. Parameters of power-law fits to the functions $N_{SFOAE}(f)$ and $Q_{ERB}(f_{CF})$ in three species. Power-law fits (i.e., straight-line approximations on log-log axes) are an excellent approximation to N_{SFOAE} at $f > 1$ kHz and to Q_{ERB} over the entire frequency range. For each species, the parameters $\{\alpha,\beta\}$ characterizing the frequency dependence of $N_{SFOAE}(f)$ and $Q_{ERB}(f_{CF})$ in the high-frequency region of the cochlea were determined by linear regression using power-law fits of the form $y = \beta x^{\alpha}$, where y is the dependent variable and $x = f/[\text{kHz}]$ (i.e., frequency or CF in kHz). The numbers in parentheses give the approximate uncertainty (i.e., 95% confidence interval) in the final digit(s) estimated from the fits [e.g., $0.44(5) = 0.44 \pm 0.05$]; when the uncertainty is 1 or greater, the position of the decimal point is shown for clarity. The uncertainties in α and $\log\beta$ are strongly correlated, with a typical correlation coefficient between them of roughly -0.9.

$\beta\ (f/[\text{kHz}])^{\alpha}$		Cat	Guinea pig	Human
N_{SFOAE}	α	0.44(5)	0.44(3)	0.37(7)
	β	3.32(36)	3.56(26)	11.0(1.2)
Q_{ERB}	α	0.37(10)	0.35(4)	—
	β	5.0(1.1)	4.0(3)	—

D. Testing the predicted covariation of Q_{ERB} and N_{SFOAE}

We test the predicted covariation of Q_{ERB} and N_{SFOAE} in Fig. 3 by replotting the group delays $\tau_{SFOAE}(f)$ from Fig. 1 in the dimensionless form $N_{SFOAE}(f)$. Comparing the functions $N_{SFOAE}(f)$ (from Fig. 3) with $Q_{ERB}(f_{CF})$ (from Fig. 2) demonstrates that in cats and guinea pigs the frequency dependence of $N_{SFOAE}(f)$ generally parallels the CF dependence of the sharpness of tuning, at least in the basal half of the cochlea. In addition, note that although SFOAE group delays *decrease* at higher frequencies when measured in fixed units of time (e.g., milliseconds, as in Fig. 1), they

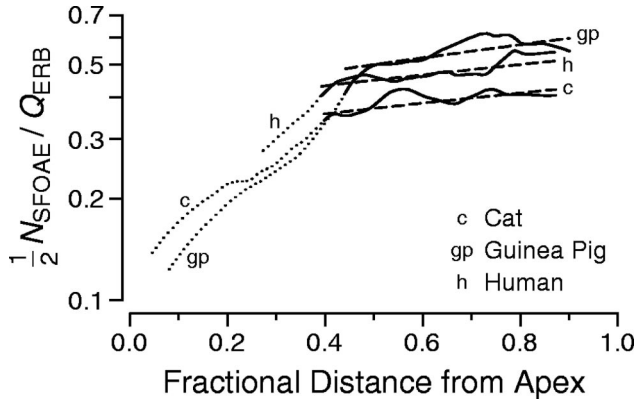

FIG. 4. Estimated tuning ratio N_{BM}/Q_{ERB} in three species. Tuning ratios were computed from the data in Figs. 2 and 3 using either the loess trend lines (solid lines) or the corresponding power-law fits (dashed lines). Values for the human Q_{ERB} were obtained by combining the otoacoustic and behavioral estimates of tuning reported by Shera *et al.* (2002; see also Oxenham and Shera, 2002). The horizontal axes represent relative cochlear location obtained by inverting the corresponding cochlear position-frequency map (Liberman, 1982; Greenwood, 1990; Tsuji and Liberman, 1997). Based on the intensity dependence of human OAE latencies reported by Neely *et al.* (1998), the values shown here may underestimate threshold-level tuning ratios by perhaps 30%, independent of frequency (see text). In the apical 40% of the cochlea, where the ratios and their dependence on frequency are of more uncertain reliability, the estimates are shown using dotted lines.

increase with frequency when measured in natural dimensionless units (i.e., periods of the stimulus waveform, as in Fig. 3). In cats, for example, the $N_{SFOAE}(f)$ trend line increases by roughly a factor of 20 from apex to base; similar variations in N_{SFOAE} are apparent in guinea pigs and humans. Given the sharpening of neural tuning at high CFs (Fig. 2), the frequency dependence of $N_{SFOAE}(f)$ demonstrated here is in qualitative agreement with expectations from filter theory about the covariation of bandwidth and group delay. Figures 2 and 3 thus support a general proportionality between N_{SFOAE} and N_{BM}, as predicted by Eq. (13).

1. The tuning ratio

The approximate proportionality between N_{SFOAE} and Q_{ERB} can be quantified by explicit calculation of the tuning ratio N_{BM}/Q_{ERB} using the theoretical estimate

$$N_{BM} \approx \tfrac{1}{2} N_{SFOAE}. \tag{15}$$

Figure 4 shows the estimated tuning ratio N_{BM}/Q_{ERB} as a function of relative cochlear location as computed from the data in Figs. 2 and 3. [Values for the human Q_{ERB} were obtained by combining the otoacoustic and behavioral estimates of tuning reported by Shera *et al.* (2002; see also Oxenham and Shera, 2002). The otoacoustic estimates of Q_{ERB} in that study were obtained by assuming approximate species-invariance of the tuning ratio (see Sec. V E 1).] Note that the values in Fig. 4 were obtained by combining measurements of N_{SFOAE} and Q_{ERB} made at somewhat different sound intensities. (The measurements of N_{SFOAE} were made at 40 dB SPL; the values of Q_{ERB} were obtained from ANF tuning curves with thresholds typically near 10 dB SPL in cat and 15 dB SPL in guinea pig.) Since OAE latencies generally decrease at higher sound levels (e.g., Neely *et al.*, 1988), the values of $\frac{1}{2}N_{SFOAE}/Q_{ERB}$ in Fig. 4 presumably underestimate the tuning ratios characteristic of threshold-level tuning. The intensity dependence of human OAE latencies reported by Neely *et al.* (1988), if generally applicable to the cat and guinea pig, suggests that the values in Fig. 4 systematically underestimate threshold-level tuning ratios by perhaps 30%.[8] (This value is likely to be an upper bound; Neely *et al.*'s characterization presumably overestimates the intensity dependence of OAE latencies at sound-levels near threshold, where cochlear mechanics is approximately linear.) Additional data are needed to determine the appropriate correction factor in each species. We focus here on the CF dependence shown in Fig. 4; since roughly the same correction applies at all frequencies (Neely *et al.*, 1988), the overall frequency dependence is largely unaffected.

Figure 4 indicates that the estimated tuning ratio behaves very differently in the base and the apex of the cochlea. In the basal 60% of the cochlea N_{BM}/Q_{ERB} increases slowly with distance from the apex, its value changing by only 20% over a region where N_{BM} and Q_{ERB} vary by at least 300%. N_{BM} and Q_{ERB} thus vary together in nearly constant proportion, as expected from filter theory and the predicted proportionality between N_{SFOAE} and N_{BM}. In the apical 40% of the cochlea, however, the tuning ratio varies more rapidly with position. This change in the form of N_{BM}/Q_{ERB} reflects a mid-frequency change in $N_{SFOAE}(f)$. Figure 3 demonstrates a "bend" in the function $N_{SFOAE}(f)$ at a frequency that maps in each species to a location just apical to the midpoint of the cochlea. The bend, a change of slope on log-log axes, represents a change in the power-law exponent. No bend or other change of form corresponding to that seen in Fig. 3 for $N_{SFOAE}(f)$ is apparent in the functions $Q_{ERB}(f_{CF})$ reproduced in Fig. 2. As a result, the bend in $N_{SFOAE}(f)$ appears also in the ratio N_{SFOAE}/Q_{ERB}, and the tuning ratio changes form. Note that because the tuning ratio varies more slowly than $N_{SFOAE}(f)$—thereby allowing an expanded vertical scale on the plot—the bend is much more salient in Fig. 4 than in Fig. 3. The strong variation of N_{BM}/Q_{ERB} in the apex may reflect either rapid changes with CF in the form of mechanical tuning (e.g., the effective order of the mechanical filter) and/or a systematic breakdown in the proportionality between otoacoustic and BM group delays [e.g., a violation of Eq. (1)]. Whatever its origin, the mid-cochlear bend in $N_{SFOAE}(f)$ assumes a remarkably similar form in all of the three species. Interestingly, the location of the bend corresponds approximately with the frequency at which cat ANF tuning curves change from the classic tip/tail form characteristic of high-CF fibers to the more complex shapes found in the apex (Liberman, 1978; Liberman and Kiang, 1978).

E. Apparent breakdown in the apex of the cochlea

Although Eq. (13) appears valid at high CFs, several pieces of evidence suggest that the relation breaks down in the apex of the cochlea. Figure 5 compares values of $N_{SFOAE}(f)$ with estimates of $2N_{BM}(f)$ obtained from mechanical and neural data at low CFs. In the cat, the N_{SFOAE} trend line and round-trip group delays estimated from auditory-nerve fibers (Goldstein *et al.*, 1971) part company at CFs below 3 kHz. At the apical end of the guinea pig

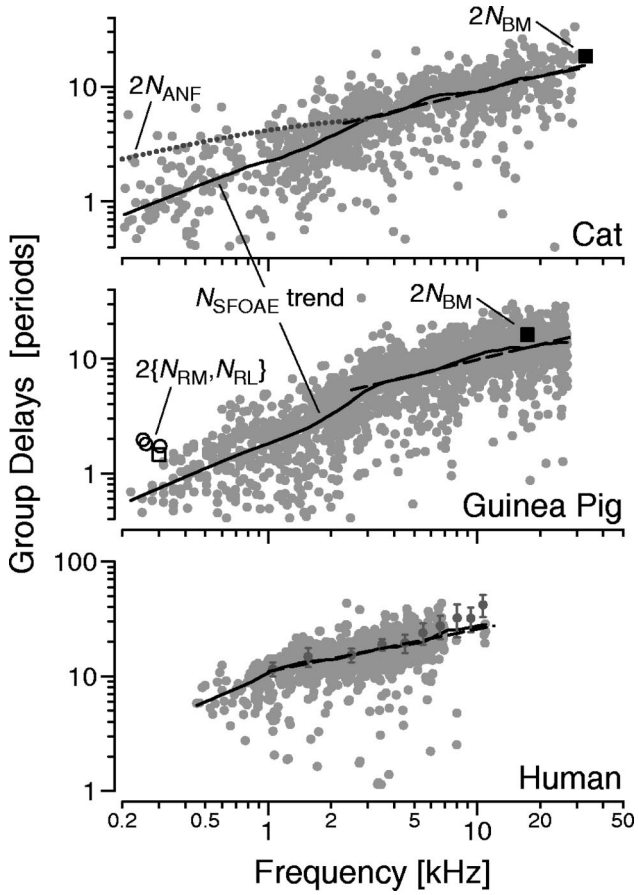

FIG. 5. N_{SFOAE} compared with mechanical and neural data in the apex. Superimposed on the data and trend lines from Fig. 3 are values of mechanical and neural group delays at low CFs. The mechanical data in the guinea pig (open symbols) were obtained from measurements on Reissner's membrane (Cooper and Rhode, 1995, □) or the reticular lamina (Khanna and Hao, 1999, ○) at high sound levels. The neural data in the cat (dotted line) is a curve fit to energy-weighted group delays obtained from auditory-nerve fiber (ANF) responses by Goldstein *et al.* (1971). The ANF values were corrected for fiber transmission delay by subtracting 1 ms. Both mechanical and neural group delays were doubled to estimate round-trip delay for comparison with N_{SFOAE}.

cochlea, similar differences between otoacoustic and mechanical group delays are seen based on measurements from Reissner's membrane (Cooper and Rhode, 1995) and the reticular lamina (Khanna and Hao, 1999). Although interpretations are complicated—both by potential problems relating neural and mechanical group delays and because the mechanical data from the apex were obtained from measurements on Reissner's membrane or the reticular lamina at high sound levels in cochleae of uncertain condition—the data suggest that $N_{\mathrm{SFOAE}}(f)$ is systematically smaller than predicted by Eq. (13) in the apex of the cochlea. Note, however, that a simple straight-line extrapolation of $N_{\mathrm{SFOAE}}(f)$ to low CFs using the slope characteristic of the high-CF region yields a curve largely consistent with the mechanical and neural data from the apex.

V. SUMMARY AND DISCUSSION

The theory of coherent reflection filtering predicts that reflection-source-emission group delay (τ_{SFOAE}) is determined by the group delay of the basilar-membrane mechanical transfer function ($\hat{\tau}_{\mathrm{BM}}$) through Eq. (1). We tested this prediction by comparing ear-canal measurements of $\tau_{\mathrm{SFOAE}}(f)$ in cats and guinea pigs with values of $2\hat{\tau}_{\mathrm{BM}}(f)$ computed from published measurements of BM transfer functions (Cooper and Rhode, 1992; Nuttall and Dolan, 1996). Although an explicit comparison is possible only at the extreme basal end of the cochlea, the mechanical and otoacoustic data appear generally consistent with the theory, especially considering the possible sources of error, and that the mechanical group delays represent only a single animal in each species. The comparison suggests, however, that the ratio $\tau_{\mathrm{SFOAE}}/\hat{\tau}_{\mathrm{BM}}$, although significantly greater than 1, may be slightly less than the value 2 predicted by the theory. Ratios somewhat less than 2 would occur if the region of wave scattering were skewed slightly basally from the peak of the traveling wave. Definitive tests of the theory using BM measurements require additional data (see Sec. V D).

A comparison between τ_{SFOAE} and $\hat{\tau}_{\mathrm{BM}}$ based on the variation in the sharpness of neural tuning with CF can be made over the entire frequency range and suggests that the proportionality $\tau_{\mathrm{SFOAE}}(f) \propto \hat{\tau}_{\mathrm{BM}}(f)$ holds in roughly the basal-most 60% of the cochlea. At low frequencies, however, the otoacoustic measurements disagree with neural and mechanical group delays from the apex of the cochlea. Human SFOAE group delays measured over a four-octave range are roughly a factor of 3 longer than their counterparts in cat and guinea pig but show similar trends across CF.

A. Global deviations from scaling

In locally scaling-symmetric cochleae, transfer functions $T(x,f)$ measured at nearby locations overlie one another when plotted as a function of the normalized frequency f/f_{CF}, where f_{CF} is the characteristic frequency (Zweig, 1976; Siebert, 1968; Sondhi, 1978). In perfectly scaling cochleae, the relative bandwidths of tuning [e.g., the functions $Q_{\mathrm{ERB}}(f_{\mathrm{CF}})$] are constant, independent of CF. Likewise, the theory of coherent reflection filtering predicts that in a perfectly scaling cochlea, SFOAE group delays—expressed in the dimensionless form $N_{\mathrm{SFOAE}}(f)$ as the number of stimulus periods—are also constant, independent of f. Although measurements of BM motion and neural tuning curves indicate that an approximate scaling symmetry applies locally (Rhode, 1971; Kiang and Moxon, 1974; Liberman, 1978), the plots of Q_{ERB} and N_{SFOAE} in Figs. 2 and 3 demonstrate global deviations from scaling whose form appears quantitatively similar in cats, guinea pigs, and humans.

We note that the systematic deviations from scaling demonstrated here imply that when the cochlear frequency-position map is logarithmic the function $T(x,f)$ cannot be symmetric about its peak in both the space and log-frequency domains simultaneously. Consider, for example, the case where the spatial envelope of the traveling wave at frequency f_0 [i.e., $|T(x,f_0)|$ vs x] is symmetric about its peak at $\hat{x}(f_0)$. Approximate symmetry about the peak of the traveling wave has recently been reported in longitudinal measurements of basilar-membrane motion (Ren, 2002). If the sharpness of frequency tuning increases with CF, other things being equal, then the amplitude of the transfer function at location $x_0 \equiv \hat{x}(f_0)$ [i.e., $|T(x_0,f)|$ vs f] must be asymmetric (on a log

TABLE II. Otoacoustic estimates of the wavelength at the peak of the traveling wave in three species. For each species, the parameters $\{\hat{\lambda}_1, \alpha\}$ characterizing the frequency dependence of $\hat{\lambda}(f_{CF}) = \hat{\lambda}_1 (f_{CF}/[\text{kHz}])^{\alpha}$ in the high-frequency region of the cochlea were computed from the parameters in Table I using the formula $\hat{\lambda} \approx l/N_{BM}$, where $N_{BM} \approx \frac{1}{2} N_{SFOAE}$ and l is the distance over which $f_{CF}(x)$ changes by a factor of e in the basal turn of the cochlea. The values of l assumed for each species were $l = \{5.2, 3.3, 7.2\}$ mm for cat, guinea pig, and human, respectively (Liberman, 1982; Tsuji and Liberman, 1997; Greenwood, 1990). As in Table I, the numbers in parentheses give the approximate uncertainty (i.e., 95% confidence interval) in the final digit(s) [e.g., $3.13(35) = 3.13 \pm 0.35$]; confidence intervals were estimated from the fits to N_{SFOAE} and do not reflect uncertainties in the values of l.

$\hat{\lambda}_1 (f_{CF}/[\text{kHz}])^{\alpha}$	Cat	Guinea pig	Human
$\hat{\lambda}_1$ [mm]	3.13(35)	1.85(15)	1.31(15)
α	−0.44(5)	−0.44(3)	−0.37(7)

frequency axis) about its peak at f_0 (i.e., CF).[9] In particular, the frequency transfer function must fall more rapidly at frequencies above CF than below. Note, however, that in addition to variations in tuning bandwidth, other, less well characterized deviations from scaling, such as possible systematic variations in transfer function height, will presumably contribute to any apparent asymmetry. Nevertheless, we note that the sign of the asymmetry in the transfer function (i.e., a steeper high-frequency slope) predicted from the variations in bandwidth reported here is similar to that measured experimentally (e.g., Robles and Ruggero, 2001; Ren, 2002).

B. Wavelength of the traveling wave

The locally scaling-symmetric form of $T(x,f)$ implies that the spatial wavelength of the traveling wave and the group delay of the transfer function [defined by partial derivatives of $\angle T$ with respect to x and f, respectively; see Eqs. (4) and (8)] are related to one another. When the cochlear position-frequency map is exponential, the wavelength and group delay at the peak are related through the equation

$$\hat{\lambda} N_{BM}/l = 1, \tag{16}$$

where l is the distance over which $f_{CF}(x)$ changes by a factor of e (Zweig and Shera, 1995). The theoretical estimate $N_{BM} \approx \frac{1}{2} N_{SFOAE}$ allows us to compute the wavelength at the peak of the traveling wave from our otoacoustic measurements and parameters of the cochlear map (e.g., Liberman, 1982; Tsuji and Liberman, 1997; Greenwood, 1990). Power-law estimates of the wavelength $\hat{\lambda}$ as a function of CF in cat, guinea pig, and human are given in Table II. The table indicates that in each of the three species $\hat{\lambda}$ decreases systematically at higher CFs at a rate of roughly 25% per octave. In humans, for example, the wavelength $\hat{\lambda}$ decreases from a value equivalent to about 130 rows of hair cells at the 1 kHz place (assuming 10 μm/row) to about 55 rows near 10 kHz.

C. Differences between base and apex

The large deviation from the predicted relation between otoacoustic and mechanical group delays [Eq. (1)] apparent at low CFs (Fig. 5) suggests that there are important differences in mechanisms of emission generation between the base and apex of the cochlea. These apparent otoacoustic differences may be related to other, more well-established differences in the mechanical and neural responses of the base and apex. For example, recent data from the guinea pig (Cooper and Dong, 2002) suggest that mechanical nonlinearities differ markedly in form and/or frequency dependence between the base and the apex. Since the suppression method used here to measure SFOAEs relies on nonlinear interactions between the probe and the suppressor to extract the emission,[10] the differences between otoacoustic and mechanical group delays in the apex may reflect changes in the form of cochlear mechanical nonlinearities with CF.

Other possibilities are suggested by the observation that mechanical and neural responses from the apex appear to result from multiple interacting mechanical drives (reviewed in Lin and Guinan, 2000). For example, auditory-nerve fibers at low CFs in cats have multi-lobed tips (Liberman and Kiang, 1978)—in their overall form apical tuning curves more nearly resemble a distorted ''W'' than the classic ''V'' shape characteristic of tuning curves from the base—and the phase-versus-frequency curves for these low-CF fibers manifest two well-defined and different group delays, separated by a transition at the ''seams'' between the lobes (Pfeiffer and Molnar, 1970; Kiang, 1984). Since different mechanical drives may couple differently to propagating pressure-difference waves and thereby produce backward-traveling waves with different characteristics, the relationship between OAEs and the motion of the organ of Corti, like the shapes of neural tuning curves, may vary systematically along the length of the cochlea. Perhaps significantly, the discrepancy between otoacoustic theory and experiment first becomes evident in cat at approximately the same frequency where neural tuning curves change from the classic tip/tail form to the more complex shapes found in the apex. Additional data and analysis are needed to explore these possibilities and to provide definitive tests of Eq. (1) in the apex.

D. Definitive tests of the theory

Rigorous tests of Eq. (1) should ideally be performed using simultaneous measurements of SFOAEs and BM motion in the same animal. In addition to eliminating uncertainty in the conclusions arising from differences among preparations, simultaneous otoacoustic and BM measurements would enable one to perform the more definitive experiment of testing the theory's prediction for the change in the reflection-source-emission spectrum caused by the introduction of artificial impedance perturbations (Zweig and Shera, 1995). For a masslike perturbation located at position x, the theory predicts that the change in the emission spectrum is proportional to $\omega T^2(x,f)$.

E. Applications of the tuning ratio

The tuning ratio N_{BM}/Q_{ERB} is equivalent to the product of BM group delay and bandwidth (as measured by the ERB); its value provides a dimensionless measure of the effective ''shape'' or ''order'' of cochlear tuning. Local scal-

ing can be used to interpret the tuning ratio in the spatial domain. The exponential form of the cochlear map implies that the spatial correlate of the ERB [sometimes called the ''equivalent rectangular spread'' or ERS (cf. Allen, 1996)] has the value $\mathrm{ERS}=l/Q_{\mathrm{ERB}}$. Combining this relation with Eq. (16) for $\hat{\lambda}$ shows that the tuning ratio, $N_{\mathrm{BM}}/Q_{\mathrm{ERB}}$, represents the ratio of the ERS to the wavelength at the peak of the traveling wave ($\mathrm{ERS}/\hat{\lambda}$).

A quantity analogous to the tuning ratio can be computed for any bandpass filter if $N_{\mathrm{BM}}(f_{\mathrm{CF}})$ is identified with the group delay at the filter peak. For example, in the family of gammatone filters widely used as models of peripheral auditory filters (e.g., Johannesma, 1972; Patterson *et al.*, 1991), the tuning ratio $N_{\mathrm{BM}}/Q_{\mathrm{ERB}}$ uniquely determines the filter order.[11] By specifying the filter order, the tuning ratio controls the asymmetry (or skewness) of the impulse-response envelope about its maximum: larger ratios correspond to higher orders, and thus to more symmetrical impulse responses (Aertsen and Johannesma, 1980).

Measurements of the tuning ratio across CF—when obtained from values of N_{SFOAE} and Q_{ERB} measured at comparable sound intensities—can thus be used to determine the characteristics of gammatone or other models of cochlear tuning. It would be instructive to compare the filter characteristics determined in this way with those obtained by fitting filter models to ANF impulse responses measured using reverse correlation (e.g., Carney and Yin, 1988). Since additional delays not directly associated with cochlear tuning (e.g., acoustic and/or neural transmission delays) are implicitly included in the definition of the revcor filter, group delays obtained otoacoustically presumably provide better estimates of mechanical group delay in the cochlea.

1. Noninvasive measurement of cochlear tuning

Rather than committing oneself to a particular type of filter (e.g., a gammatone), one can apply the tuning ratio to estimate the frequency selectivity of cochlear tuning in a more model-independent manner (Shera *et al.*, 2002). The method is based on the assumption that at corresponding cochlear locations the tuning ratio is broadly similar across mammalian species. If this assumption is correct (e.g., if the analytic structure of mammalian mechanical transfer functions is approximately conserved across species), then noninvasive estimates of the human Q_{ERB} can be obtained by combining otoacoustic estimates of the human N_{BM} with the tuning ratios measured in cat and/or guinea pig. More precisely,

$$Q_{\mathrm{ERB}}^{\mathrm{human}} \approx k_{\mathrm{gpig}} N_{\mathrm{BM}}^{\mathrm{human}}, \tag{17}$$

where $k_{\mathrm{gpig}} \equiv Q_{\mathrm{ERB}}^{\mathrm{gpig}}/N_{\mathrm{BM}}^{\mathrm{gpig}}$ is the reciprocal of the guinea-pig tuning ratio obtained by combining otoacoustic and neurophysiological measurements as in Fig. 4. Note that so long as the otoacoustic measurements are made at comparable sound intensities in the two species (in this example, human and guinea pig), systematic errors due to differences in the intensities at which N_{SFOAE} and Q_{ERB} are measured will, to first order, cancel in the product. [For example, if $N_{\mathrm{SFOAE}}^{\mathrm{gpig}}$ and $N_{\mathrm{SFOAE}}^{\mathrm{human}}$ measured at 40 dB SPL both differ by roughly the same (unknown, possibly frequency dependent) factor from their values near threshold, then the unknown factors cancel out when computing $Q_{\mathrm{ERB}}^{\mathrm{human}}$ from Eq. (17).]

We apply these ideas in another publication (Shera *et al.*, 2002), in which we combine the theory of coherent reflection filtering with otoacoustic measurements to compare cochlear tuning across species and to test the correspondence between physiological and behavioral measures of auditory frequency selectivity. The results indicate that, contrary to common belief, tuning in the human cochlea is considerably sharper than that found in the other mammals. In addition, at low sound levels human cochlear tuning appears to be more than twice as sharp as implied by standard behavioral studies and has a different dependence on frequency. These findings are consistent with new behavioral measurements designed to minimize the influence of nonlinear effects such as suppression (Oxenham and Shera, 2002). The measurements and analysis reported here thus illustrate the rich potential inherent in OAEs for obtaining valuable new information about basic cochlear properties.

ACKNOWLEDGMENTS

We thank Nigel P. Cooper, M. Charles Liberman, and Alfred L. Nuttall for generously sharing their data, Jont B. Allen and Andrew J. Oxenham for stimulating discussions, and Paul F. Fahey, K. Domenica Karavitaki, William T. Peake, and Robert H. Withnell for valuable comments on the manuscript. This work was supported by Grant Nos. DC03687 and DC00235 from the NIDCD, National Institutes of Health.

[1]Preliminary accounts of this work have been presented elsewhere (Shera and Guinan, 2000a, b).

[2]Alternative derivations of Eq. (1) are available elsewhere (Shera, 1992; Zweig and Shera, 1995; Talmadge *et al.*, 1998).

[3]By characterizing the middle-ear using transmittance and reflectance coefficients (Shera and Zweig, 1992), one can easily show that the SFOAE pressure, P_{SFOAE}, has the value

$$P_{\mathrm{SFOAE}} = P_0 \vec{T}_{\mathrm{me}} \overleftarrow{T}_{\mathrm{me}} \frac{R(1+R_{\mathrm{stapes}})}{1-RR_{\mathrm{stapes}}},$$

where P_0 is the calibrated ear-canal stimulus pressure, $\vec{T}_{\mathrm{me}}$ and $\overleftarrow{T}_{\mathrm{me}}$ are, respectively, the forward and reverse middle-ear pressure transfer functions, R_{stapes} is the reflection coefficient for retrograde cochlear waves at the stapes (Shera and Zweig, 1991; Talmadge *et al.*, 1998; Puria, 2002), and R is the cochlear traveling-wave reflectance (Shera and Zweig, 1993a; Zweig and Shera, 1995; Talmadge *et al.*, 1998), defined as the ratio of the emitted (backward-traveling) to the stimulus (forward-traveling) pressure wave at the stapes. Note that P_0, $\vec{T}_{\mathrm{me}}$, and $\overleftarrow{T}_{\mathrm{me}}$ are measured at sound intensities where $|P_{\mathrm{SFOAE}}/P_0| \ll 1$. Noncochlear contributions to τ_{SFOAE} are small when $\angle R$ dominates the frequency dependence of $\angle P_{\mathrm{SFOAE}}$.

[4]The value of τ_{SFOAE} used to compute the ratio was obtained using the power-law fits given in Table I.

[5]Measurements of ANF group delay in fibers with CFs near 12 kHz have been obtained in the guinea pig using responses to amplitude-modulated tones (Gummer and Johnstone, 1984). The authors of that study argue that the ''group delay difference,'' obtained as the difference between the near-CF group delay and the group delay measured about one octave below CF, correlates well with the sharpness of tuning measured using the Q_{10}. Although the group delay differences reported for their most sensitive units agree well with our values of τ_{SFOAE} near 12 kHz in the guinea pig, we do not show these neural data here because of our uncertainty about the interpretation of the delay difference, especially in light of other measurements suggesting that neural group delays at tail frequencies often have a nonmonotonic frequency dependence (e.g., Allen, 1983). See also van der

Heijden and Joris (2002) for another method to estimate high-frequency phase characteristics from ANF responses to complex stimuli.

[6]Although we adopt the ERB-based measure to facilitate comparisons with behavioral measurements, we obtain similar conclusions using Q_{10}, defined as f_{CF}/BW_{10}, where BW_{10} is the bandwidth 10 dB below the peak. In many filters the two measures are simply proportional: for simple harmonic oscillators $Q_{ERB}/Q_{10}\approx 1.9$, and for Gaussian filters $Q_{ERB}/Q_{10}\approx 1.7$. Analysis of ANF tuning curves (Shera, unpublished) yields similar ratios (i.e., $Q_{ERB}/Q_{10}\approx 1.7-1.8$), largely independent of species and CF.

[7]Thanks to Jont Allen for suggesting this formulation.

[8]According to the measurements and analysis of Neely *et al.* (1988), evoked OAE latencies measured at sound level $L+\Delta L$ (in dB SPL) will differ from those measured at level L by a frequency-independent factor of approximately $c^{-\Delta L/100}$, with $c=5$.

[9]As a convenient example, consider the simple Gaussian envelope

$$|T(x,f)|\propto \exp\left[\frac{x-\hat{x}(f)}{\sqrt{2}\sigma_x(f)}\right]^2,$$

where the frequency-position map $\hat{x}(f)$ is proportional to $-\log(f)$ and the width of the excitation pattern, $\sigma_x(f)$, varies with frequency. Although $|T|$ is symmetric when considered as a function of x at fixed f (the traveling wave), the function is asymmetric when considered as a function of $\log(f)$ at fixed x (the transfer function).

[10]We note the need for caution when interpreting OAE measurements obtained using the suppression method and other techniques based on nonlinear effects such as compression. As an extreme example, consider the thought experiment in which the mechanics in some region of the cochlea (e.g., the apex) is presumed completely linear. Although this region might generate strong reflection-source OAEs—the absence of nonlinearity implies neither the lack of traveling-wave amplification nor the absence of emissions—suppression and other nonlinear OAE methods would be unable to measure them. If measurable emissions at corresponding frequencies are found using these methods, then they must have come from other (nonlinear) regions of the cochlea. Similar remarks apply to the method of efferent suppression if the effective strength of efferent feedback varies strongly with position in the cochlea [as suggested, for example, by the relative sparsity of medial efferent innervation in the apex (Guinan *et al.*, 1984)].

[11]For a gammatone filter of order n

$$N_{BM}/Q_{ERB}=\tfrac{1}{2}n\Gamma(2n-1)[2^{-(n-1)}/\Gamma(n)]^2$$

(see, e.g., Aertsen and Johannesma, 1980; Hartmann, 1997). Note that all gammatone filters must satisfy $N_{BM}/Q_{ERB}\geqslant\frac{1}{2}$.

Aertsen, A. M. H. J., and Johannesma, P. I. M. (**1980**). ''Spectro-temporal receptive fields of auditory neurons in the grassfrog. I. Characterization of tonal and natural stimuli,'' Biol. Cybern. **38**, 223–234.

Allen, J. B. (**1983**). ''Magnitude and phase-frequency response to single tones in the auditory nerve,'' J. Acoust. Soc. Am. **73**, 2071–2092.

Allen, J. B. (**1996**). ''Harvey Fletcher's role in the creation of communication acoustics,'' J. Acoust. Soc. Am. **99**, 1825–1839.

Apostol, T. M. (**1969**). *Calculus*, 2nd ed. (Wiley, New York), Vol. II.

Bredberg, G. (**1968**). ''Cellular patterns and nerve supply of the human organ of Corti,'' Acta Oto-Laryngol., Suppl. **236**, 1–135.

Brillouin, L. (**1946**). *Wave Propagation in Periodic Structures* (McGraw-Hill, New York).

Carney, L. H., and Yin, T. C. T. (**1988**). ''Temporal coding of resonances by low-frequency auditory nerve fibers: Single fiber responses and a population model,'' J. Neurophysiol. **60**, 1653–1677.

Cleveland, W. S. (**1993**). *Visualizing Data* (Hobart, Summit, NJ).

Cooper, N. P., and Dong, W. (**2002**). ''Baseline position shifts and mechanical compression in the apical turns of the cochlea,'' in *Biophysics of the Cochlea: From Molecule to Model*, edited by A. W. Gummer (World Scientific, Singapore), pp. 157–163.

Cooper, N. P., and Rhode, W. S. (**1992**). ''Basilar membrane mechanics in the hook region of cat and guinea-pig cochleae: Sharp tuning and nonlinearity in the absence of baseline position shifts,'' Hear. Res. **63**, 163–190.

Cooper, N. P., and Rhode, W. S. (**1995**). ''Nonlinear mechanics at the apex of the guinea-pig cochlea,'' Hear. Res. **82**, 225–243.

de Boer, E. (**1997**). ''Cochlear models and minimum phase,'' J. Acoust. Soc. Am. **102**, 3810–3813.

Dreisbach, L. E., Siegel, J. H., and Chen, W. (**1998**). ''Stimulus-frequency otoacoustic emissions measured at low and high frequencies in untrained human subjects,'' Assoc. Res. Otolaryngol. Abs. **21**, 349.

Engström, H., Ades, H. W., and Andersson, A. (**1966**). *Structural Pattern of the Organ of Corti* (Williams and Wilkins, Baltimore).

Evans, E. F., and Wilson, J. P. (**1973**). ''Frequency selectivity in the cochlea,'' in *Basic Mechanisms in Hearing*, edited by A. R. Møller and P. Boston (Academic, New York), pp. 519–551.

Goldstein, J. L., Baer, T., and Kiang, N. Y. S. (**1971**). ''A theoretical treatment of latency, group delay, and tuning characteristics of auditory-nerve responses to clicks and tones,'' in *Physiology of the Auditory System*, edited by M. B. Sachs (National Educational Consultants, Baltimore), pp. 133–141.

Greenwood, D. D. (**1990**). ''A cochlear frequency-position function for several species—29 years later,'' J. Acoust. Soc. Am. **87**, 2592–2605.

Guinan, J. J. (**1986**). ''Effect of efferent neural activity on cochlear mechanics,'' Scand. Audiol. Suppl. **25**, 53–62.

Guinan, J. J., Warr, W. B., and Norris, B. E. (**1984**). ''Topographic organization of the olivocochlear projections from the lateral and medial zones of the superior olivary complex,'' J. Comp. Neurol. **226**, 21–27.

Gummer, A. W., and Johnstone, B. M. (**1984**). ''Group delay measurements from spiral ganglion cells in the basal turn of the guinea pig cochlea,'' J. Acoust. Soc. Am. **76**, 1388–1400.

Hartmann, W. M. (**1997**). *Signal, Sound, and Sensation* (AIP, Woodbury).

Johannesma, P. I. M. (**1972**). ''The pre-response stimulus ensemble of neurons in the cochlear nucleus,'' in *Hearing Theory 1972* (Institute for Perception Research, Eindhoven), pp. 58–69.

Kemp, D. T. (**1978**). ''Stimulated acoustic emissions from within the human auditory system,'' J. Acoust. Soc. Am. **64**, 1386–1391.

Kemp, D. T. (**1980**). ''Towards a model for the origin of cochlear echoes,'' Hear. Res. **2**, 533–548.

Kemp, D. T. (**1986**). ''Otoacoustic emissions, travelling waves and cochlear mechanisms,'' Hear. Res. **22**, 95–104.

Khanna, S. M., and Hao, L. F. (**1999**). ''Reticular lamina vibrations in the apical turn of a living guinea pig cochlea,'' Hear. Res. **132**, 15–33.

Kiang, N. Y. S. (**1984**). ''Peripheral neural processing of auditory information,'' in *Handbook of Physiology, Section 1: The Nervous System, Vol. 3 (Sensory Processes)*, edited by I. Darian-Smith (American Physiological Society, Bethesda), pp. 639–674.

Kiang, N. Y. S., and Moxon, E. C. (**1974**). ''Tails of tuning curves of auditory-nerve fibers,'' J. Acoust. Soc. Am. **55**, 620–630.

Liberman, M. C. (**1978**). ''Auditory-nerve response from cats raised in a low-noise chamber,'' J. Acoust. Soc. Am. **63**, 442–455.

Liberman, M. C. (**1982**). ''The cochlear frequency map for the cat: Labeling auditory-nerve fibers of known characteristic frequency,'' J. Acoust. Soc. Am. **72**, 1441–1449.

Liberman, M. C. (**1990**). ''Effects of chronic cochlear de-efferentation on auditory-nerve response,'' Hear. Res. **49**, 209–224.

Liberman, M. C., and Kiang, N. Y. S. (**1978**). ''Acoustic trauma in cats: Cochlear pathology and auditory-nerve activity,'' Acta Oto-Laryngol., Suppl. **358**, 1–63.

Lighthill, J. (**1981**). ''Energy flow in the cochlea,'' J. Fluid Mech. **106**, 149–213.

Lin, T., and Guinan, J. J. (**2000**). ''Auditory-nerve-fiber responses to high-level clicks: Interference patterns indicate that excitation is due to the combination of multiple drives,'' J. Acoust. Soc. Am. **107**, 2615–2630.

Lonsbury-Martin, B. L., Martin, G. K., Probst, R., and Coats, A. C. (**1988**). ''Spontaneous otoacoustic emissions in the nonhuman primate. II. Cochlear anatomy,'' Hear. Res. **33**, 69–94.

Narayan, S. S., Temchin, A. N., Recio, A., and Ruggero, M. A. (**1998**). ''Frequency tuning of basilar membrane and auditory nerve in the same cochleae,'' Science **282**, 1882–1884.

Neely, S. T., Norton, S. J., Gorga, M. P., and Jesteadt, W. (**1988**). ''Latency of auditory brain-stem responses and otoacoustic emissions using tone-burst stimuli,'' J. Acoust. Soc. Am. **83**, 652–656.

Norton, S. J., and Neely, S. T. (**1987**). ''Tone-burst-evoked otoacoustic emissions from normal-hearing subjects,'' J. Acoust. Soc. Am. **81**, 1860–1872.

Nuttall, A. L., and Dolan, D. F. (**1996**). ''Steady-state sinusoidal velocity responses of the basilar membrane in guinea pig,'' J. Acoust. Soc. Am. **99**, 1556–1565.

Olson, E. S. (**1998**). ''Observing middle and inner ear mechanics with novel intra-cochlear pressure sensors,'' J. Acoust. Soc. Am. **103**, 3445–3463.

Oxenham, A. J., and Shera, C. A. (**2002**). ''Estimates of human cochlear

tuning at low levels using forward and simultaneous masking,'' J. Assoc. Res. Otolaryngol. (in press).
Patterson, R. D., Holdsworth, J., Nimmo-Smith, I., and Rice, P. (**1991**). ''The auditory filter bank,'' MRC-APU Report 2341, Cambridge, England.
Pfeiffer, R. R., and Molnar, C. E. (**1970**). ''Cochlear nerve fiber discharge patterns: Relationship to the cochlear microphonic,'' Science **167**, 1614–1616.
Press, W. H., Teukolsky, S. A., Vetterling, W. T., and Flannery, B. P. (**1992**). *Numerical Recipes in C: The Art of Scientific Computing* (Cambridge U.P., Cambridge).
Puria, S. (**2002**). ''Measurements of human middle ear forward and reverse acoustics: Implications for otoacoustic emissions,'' J. Acoust. Soc. Am. (in press).
Puria, S., and Allen, J. (**1998**). ''Measurements and model of the cat middle ear: Evidence of tympanic membrane acoustic delay,'' J. Acoust. Soc. Am. **104**, 3463–3481.
Ren, T. (**2002**). ''Longitudinal pattern of basilar membrane vibration in the sensitive cochlea,'' Proc. Natl. Acad. Sci. U.S.A. **99**, 17101–17106.
Rhode, W. S. (**1971**). ''Observations of the vibration of the basilar membrane in squirrel monkeys using the Mössbauer technique,'' J. Acoust. Soc. Am. **49**, 1218–1231.
Robles, L., and Ruggero, M. A. (**2001**). ''Mechanics of the mammalian cochlea,'' Physiol. Rev. **81**, 1305–1352.
Shera, C. A. (**1992**). ''Listening to the Ear,'' Ph.D. thesis, California Institute of Technology.
Shera, C. A., and Guinan, J. J. (**1999**). ''Evoked otoacoustic emissions arise by two fundamentally different mechanisms: A taxonomy for mammalian OAEs,'' J. Acoust. Soc. Am. **105**, 782–798.
Shera, C. A., and Guinan, J. J. (**2000a**). ''Frequency dependence of stimulus-frequency-emission phase: Implications for cochlear mechanics,'' in *Recent Developments in Auditory Mechanics*, edited by H. Wada, T. Takasaka, K. Ikeda, K. Ohyama, and T. Koike (World Scientific, Singapore), pp. 381–387.
Shera, C. A., and Guinan, J. J. (**2000b**). ''Reflection-emission phase: A test of coherent reflection filtering and a window on cochlear tuning,'' Assoc. Res. Otolaryngol. Abs. **23**, 545.
Shera, C. A., and Zweig, G. (**1991**). ''Reflection of retrograde waves within the cochlea and at the stapes,'' J. Acoust. Soc. Am. **89**, 1290–1305.
Shera, C. A., and Zweig, G. (**1992**). ''Analyzing reverse middle-ear transmission: Noninvasive Gedankenexperiments,'' J. Acoust. Soc. Am. **92**, 1371–1381.
Shera, C. A., and Zweig, G. (**1993a**). ''Noninvasive measurement of the cochlear traveling-wave ratio,'' J. Acoust. Soc. Am. **93**, 3333–3352.
Shera, C. A., and Zweig, G. (**1993b**). ''Order from chaos: Resolving the paradox of periodicity in evoked otoacoustic emission,'' in *Biophysics of Hair Cell Sensory Systems*, edited by H. Duifhuis, J. W. Horst, P. van Dijk, and S. M. van Netten (World Scientific, Singapore), pp. 54–63.
Shera, C. A., Guinan, J. J., and Oxenham, A. J. (**2002**). ''Revised estimates of human cochlear tuning from otoacoustic and behavioral measurements,'' Proc. Natl. Acad. Sci. U.S.A. **99**, 3318–2232.
Shera, C. A., Talmadge, C. L., and Tubis, A. (**2000**). ''Interrelations among distortion-product phase-gradient delays: Their connection to scaling symmetry and its breaking,'' J. Acoust. Soc. Am. **108**, 2933–2948.
Siebert, W. M. (**1968**). ''Stimulus transformations in the peripheral auditory system,'' in *Recognizing Patterns*, edited by P. A. Kolers and M. Eden (MIT, Cambridge), pp. 104–133.
Sisto, R., and Moleti, A. (**2002**). ''On the frequency dependence of the otoacoustic emission latency in hypoacoustic and normal ears,'' J. Acoust. Soc. Am. **111**, 297–308.
Sondhi, M. M. (**1978**). ''Method for computing motion in a two-dimensional cochlear model,'' J. Acoust. Soc. Am. **63**, 1468–1477.
Strube, H. W. (**1989**). ''Evoked otoacoustic emissions as cochlear Bragg reflections,'' Hear. Res. **38**, 35–45.
Talmadge, C. L., Tubis, A., Long, G. R., and Piskorski, P. (**1998**). ''Modeling otoacoustic emission and hearing threshold fine structures,'' J. Acoust. Soc. Am. **104**, 1517–1543.
Tsuji, J., and Liberman, M. C. (**1997**). ''Intracellular labeling of auditory nerve fibers in guinea pig: Central and peripheral projections,'' J. Comp. Neurol. **381**, 188–202.
van der Heijden, M., and Joris, P. X. (**2002**). ''Retrieving cochlear phase characteristics from high-frequency auditory nerve fibers,'' Assoc. Res. Otolaryngol. Abs. **25**, 329.
Wilson, J. P. (**1980**). ''Evidence for a cochlear origin for acoustic re-emissions, threshold fine-structure and tonal tinnitus,'' Hear. Res. **2**, 233–252.
Wright, A. A. (**1984**). ''Dimensions of the cochlear stereocilia in man and in guinea pig,'' Hear. Res. **13**, 89–98.
Zweig, G. (**1976**). ''Basilar membrane motion,'' in *Cold Spring Harbor Symposia on Quantitative Biology, Volume XL, 1975* (Cold Spring Harbor Laboratory, Cold Spring Harbor, NY), pp. 619–633.
Zweig, G., and Shera, C. A. (**1995**). ''The origin of periodicity in the spectrum of evoked otoacoustic emissions,'' J. Acoust. Soc. Am. **98**, 2018–2047.
Zwicker, E. (**1989**). ''Otoacoustic emissions and cochlear travelling waves,'' in *Cochlear Mechanisms—Structure, Function, and Models*, edited by J. P. Wilson and D. T. Kemp (Plenum, New York), pp. 359–366.
Zwicker, E., and Manley, G. (**1981**). ''Acoustical responses and suppression-period patterns in guinea pigs,'' Hear. Res. **4**, 43–52.